

COMPLEX OUTDOOR SOUND PROPAGATION THEORY VERSUS SCALE MODEL MEASUREMENTS

PACS REFERENCE: 43.28.FP

Premat Eric; Defrance Jérôme
Centre Scientifique et Technique du Bâtiment
24, rue Joseph Fourier
38400 Saint-Martin-d'Hères
France
Tel: (33)476762525
Fax: (33)476442046
E-mail: e.premat@cstb.fr

ABSTRACT

In this paper, complex outdoor sound propagation is investigated, involving uneven topography, obstacles, impedance discontinuities and wind and temperature gradients. The theoretical description is based on a Boundary Element Method accounting for any kind of shape and absorption of the domain boundaries while the meteorological effects are included via the Green function (Meteo-BEM model). Results coming from this approach are compared to experimental data obtained above curved scale models under controlled conditions in laboratory. The agreement between theoretical and experimental data is good. These results point out the importance of meteorological effects in complex outdoor sound propagation prediction.

1- INTRODUCTION

There is a need today of sound prediction at long ranges [1]. For these distances, on one hand meteorological effects (wind and temperature gradients, turbulence) have to be accounted for, and on the other hand, the ground appears to be often uneven. Consequently models for complex outdoor sound propagation are needed.

For this purpose, the Boundary Element Method [2] brings out a powerful solution, that has to be adapted to an atmosphere where the sound speed profile is no more constant. Using the appropriate Green function of the problem allows then meteorological effects to be taken into account in a BEM [3]. The Meteo-BEM model based on this approach has already been presented elsewhere [4, 5].

As a consequence of the development of sophisticated numerical models, reference results are needed in order to yield a basis for validation of these advanced tools. If one chooses to validate the theoretical results with outdoor measured data, variations due to the complex fluctuations of the outdoor sound field may cause large discrepancies between predicted and measured levels. In order to overcome this problem, a smart solution relies on the use of scale models in laboratory where all the parameters can be more easily controlled [6]. The curvature of the acoustic rays due to refraction effects can then be accounted for by the curvature of the scale models surfaces. Therefore an extensive measurement campaign above scale models has been undertaken at CSTB. This paper presents some results and comparisons between theory and measurements from the achieved indoor experimental database, for the case of

sound propagation above an impedance discontinuity both in a homogeneous and a downward refracting atmosphere.

2- THE IMPEDANCE DISCONTINUITY PROBLEM

A source and a receiver are located above a flat ground which is made up of two half-planes of admittance β_1 and β_2 . The reflective part of the ground (β_1 admittance) is called Γ (fig. 1). The air is firstly considered as a homogeneous fluid, then the case of the impedance discontinuity in the presence of downward refraction is investigated (for a positive constant sound speed profile).

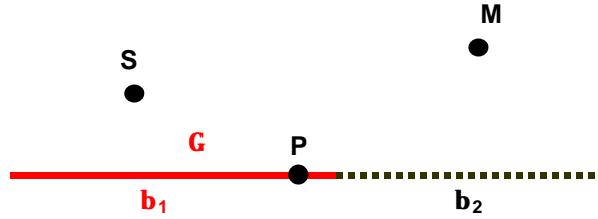


Fig. 1. Geometry of the impedance discontinuity problem

A solution of this problem for the case of an infinitely long coherent line source parallel to the impedance discontinuity has already been presented elsewhere [7, 8]. It is based on the Boundary Element Method and relies on the following integral formulation:

$$p(S, M) = G_{\beta_2}(S, M) + ik(\beta_2 - \beta_1) \int_{\Gamma} G_{\beta_2}(M, P) p(S, P) d\Gamma(P)$$

where p is the acoustic pressure, k represents the wave number, S the source and M the receiver. G_{β_1} , respectively G_{β_2} , denotes the Green function for the acoustic field above a flat boundary of homogeneous admittance β_1 , respectively β_2 . In the case of downward refraction and for a positive constant sound speed profile, the Normal Modes solution [9] can be used for the Green function of the problem allowing meteorological as well as ground effects to be accounted for.

3- THE EXPERIMENTAL SET-UP

In order to give a reference for the validation of the theoretical approach an experimental database has been built up under controlled conditions in laboratory above curved 1/20 scale models. Complex noise traffic noise problems have been investigated, involving sound propagation from low height sources above impedance discontinuities in the presence of meteorological effects.

The refracting effects are introduced using the analogy between sound propagation above flat surfaces along curved ray paths and sound propagation above curved surfaces following straight ray paths [10]. The case of downward refraction for a positive constant sound speed profile ($c(z) = c_0(1 + 0.098z)$) can be represented by a concave cylindrical surface [6] with a ray of curvature $R_c = 10.2\text{m}$ (fig. 2).

At the 1/20th scale, a felt is used in order to model a grass-like ground, whereas a polystyrene sheet has been settled for accounting for the reflective part of the surface. Using Delany and Bazley's formulation [11], the flow resistivity of the felt at the 1/20th scale is $\sigma = 3600 \text{ kNsm}^{-4}$ corresponding at full scale to a grass-like ground with $\sigma = 180 \text{ kNsm}^{-4}$. The sound pressure levels relative to the free field have been measured with the Time Delay Spectrometry technique [12]. The frequency range for the scale mode measurements is [1000 Hz, 20000 Hz]

which corresponds at full scale to [50 Hz, 1000 Hz]. It has to be pointed out that the ray of curvature of the scale model concave surface $R_c = 10.2\text{m}$ being equivalent at full scale to $R_c = 204\text{m}$ has been chosen to be smaller (stronger refraction) than in usual actual outdoor sound propagation cases in order to bring to the fore significant phenomena and to emphasize potential limitations of the theoretical models.

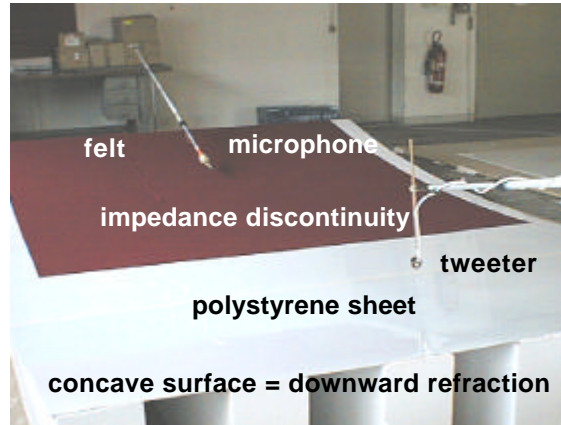


Fig. 2. Experimental set-up for the scale model of the concave surface with the impedance discontinuity

4- RESULTS AND COMPARISONS

The results of the above-mentioned theoretical approach have been compared in terms of sound pressure levels relative to the free field to experimental data obtained for a homogeneous (figures a) and an inhomogeneous medium (figures b). In order to point out the importance of refracting effects, the same configurations have been studied for both meteorological conditions. At full scale the ray curvature is $R_c = 204\text{m}$ and the flow resistivity of the absorbing part of the ground is $\sigma = 180\text{ kNsm}^{-4}$ [11].

Figures 3 to 5 show configurations that can be encountered in traffic noise studies where the source is close to the reflective ground surrounded by a grass-like surface and where the impedance jump is at the border of the road. Figures 6 and 7 give two examples of a source and a receiver at the same height, the impedance discontinuity being located 4 m from the source. In figures 8 to 10, the geometrical configuration is the same ($z_s = z_r = 2\text{ m}$, $r = 40\text{ m}$) and only the separation between source and discontinuity varies from 2 m to 28 m.

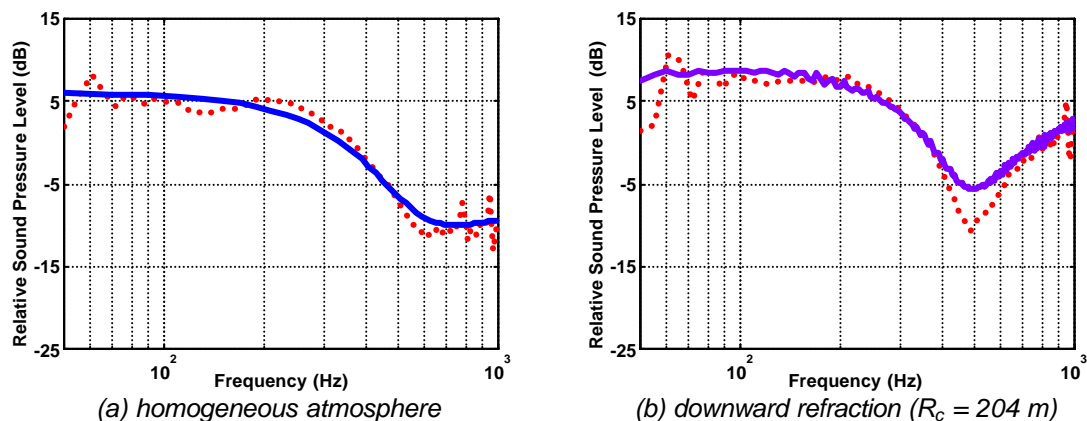
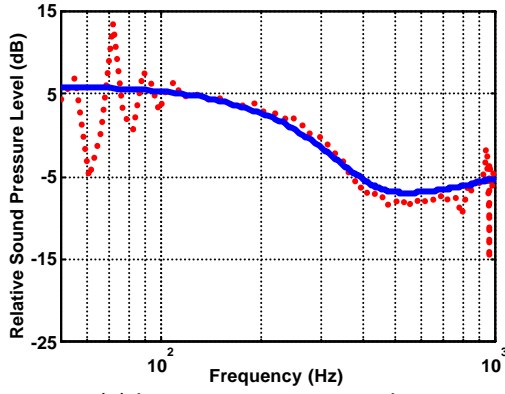
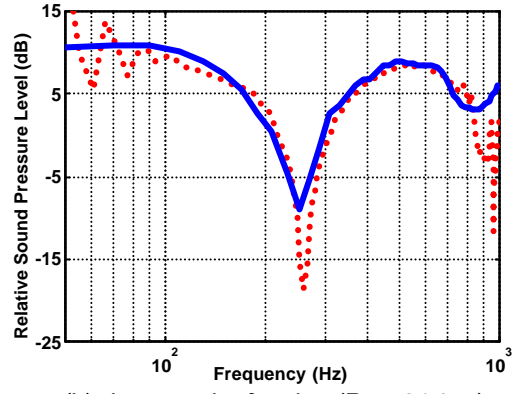


Fig. 3. Comparison theoretical model/ measurements for the surface with the impedance discontinuity, $(\underline{s}_1, \underline{s}_2) = (\underline{\mu} 180\text{ kNsm}^{-4})$, $z_s = 0.2\text{ m}$, $z_r = 1\text{ m}$, $r = 40\text{ m}$, distance between source and discontinuity = 4 m, TDS measurements — theoretical model.

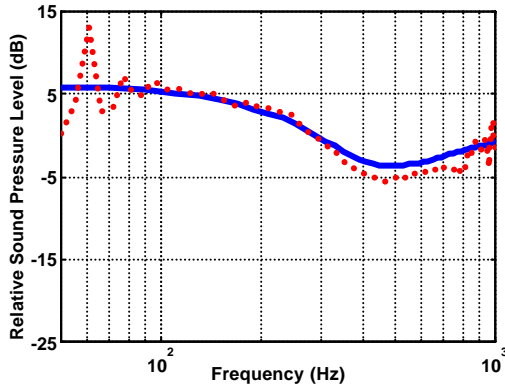


(a) homogeneous atmosphere

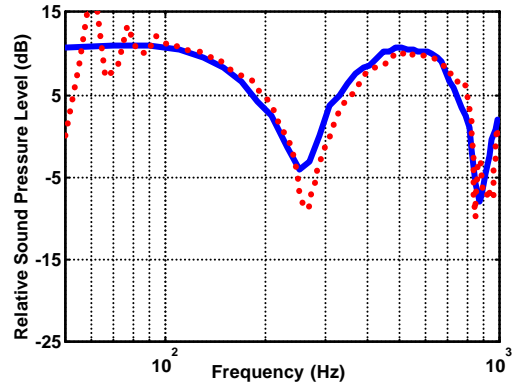


(b) downward refraction ($R_c = 204$ m)

Fig. 4. Comparison theoretical model/ measurements for the surface with the impedance discontinuity, $(\underline{s}, \underline{s}) = (\underline{\mu} 180 \text{ kNsm}^{-4})$, $z_s = 0.2$ m, $z_r = 2$ m, $r = 70$ m, distance between source and discontinuity = 8 m, TDS measurements — theoretical model.

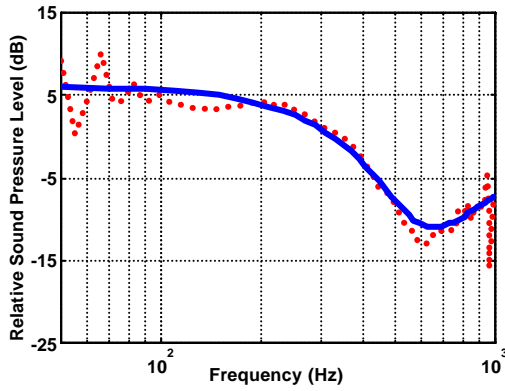


(a) homogeneous atmosphere

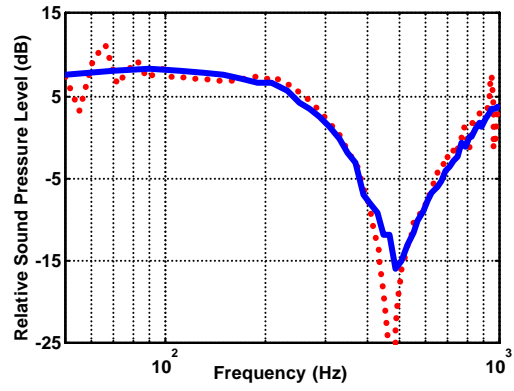


(b) downward refraction ($R_c = 204$ m)

Fig. 5. Comparison theoretical model/ measurements for the surface with the impedance discontinuity, $(\underline{s}, \underline{s}) = (\underline{\mu} 180 \text{ kNsm}^{-4})$, $z_s = 0.2$ m, $z_r = 2$ m, $r = 70$ m, distance between source and discontinuity = 20 m, TDS measurements — theoretical model.

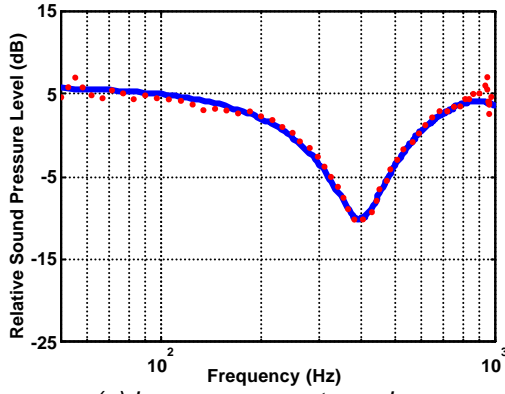


(a) homogeneous atmosphere

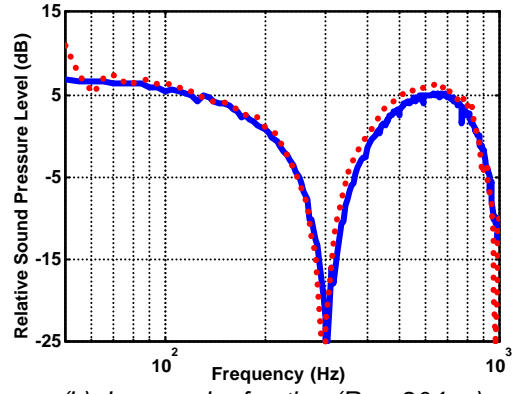


(b) downward refraction ($R_c = 204$ m)

Fig. 6. Comparison theoretical model/ measurements for the surface with the impedance discontinuity, $(\underline{s}, \underline{s}) = (\underline{\mu} 180 \text{ kNsm}^{-4})$, $z_s = 1$ m, $z_r = 1$ m, $r = 40$ m, distance between source and discontinuity = 8 m, TDS measurements — theoretical model.

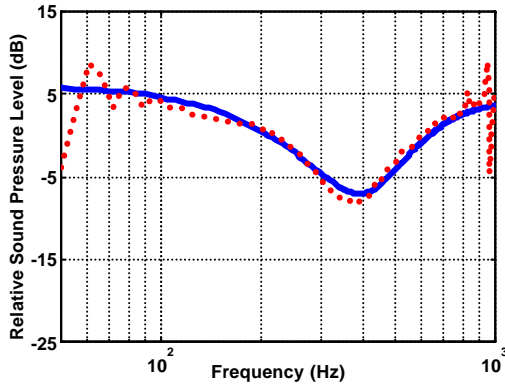


(a) homogeneous atmosphere

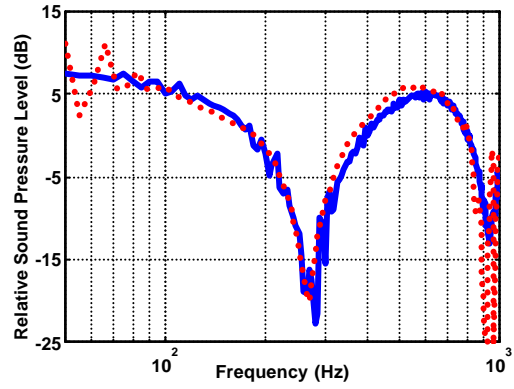


(b) downward refraction ($R_c = 204$ m)

Fig. 7. Comparison theoretical model/ measurements for the surface with the impedance discontinuity, $(\underline{S}, \underline{S}) = (\underline{\mu} 180 \text{ kNsm}^{-4})$, $z_s = 2$ m, $z_r = 2$ m, $r = 28$ m, distance between source and discontinuity = 8 m, TDS measurements — theoretical model.

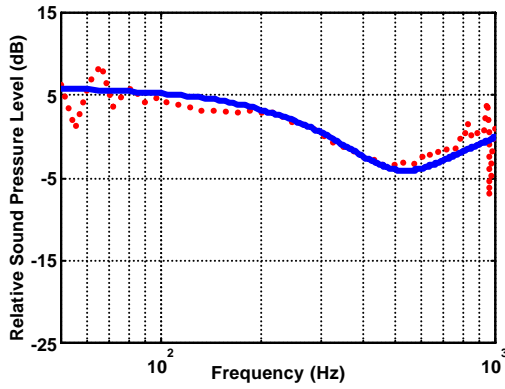


(a) homogeneous atmosphere

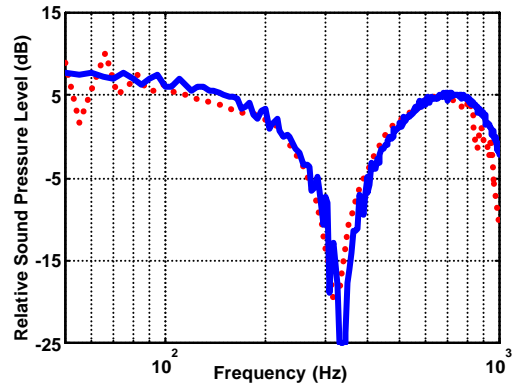


(b) downward refraction ($R_c = 204$ m)

Fig. 8. Comparison theoretical model/ measurements for the surface with the impedance discontinuity, $(\underline{S}, \underline{S}) = (\underline{\mu} 180 \text{ kNsm}^{-4})$, $z_s = 2$ m, $z_r = 2$ m, $r = 40$ m, distance between source and discontinuity = 2 m, TDS measurements — theoretical model.



(a) homogeneous atmosphere



(b) downward refraction ($R_c = 204$ m)

Fig. 9. Comparison theoretical model/ measurements for the surface with the impedance discontinuity, $(\underline{S}, \underline{S}) = (\underline{\mu} 180 \text{ kNsm}^{-4})$, $z_s = 2$ m, $z_r = 2$ m, $r = 40$ m, distance between source and discontinuity = 20 m, TDS measurements — theoretical model.

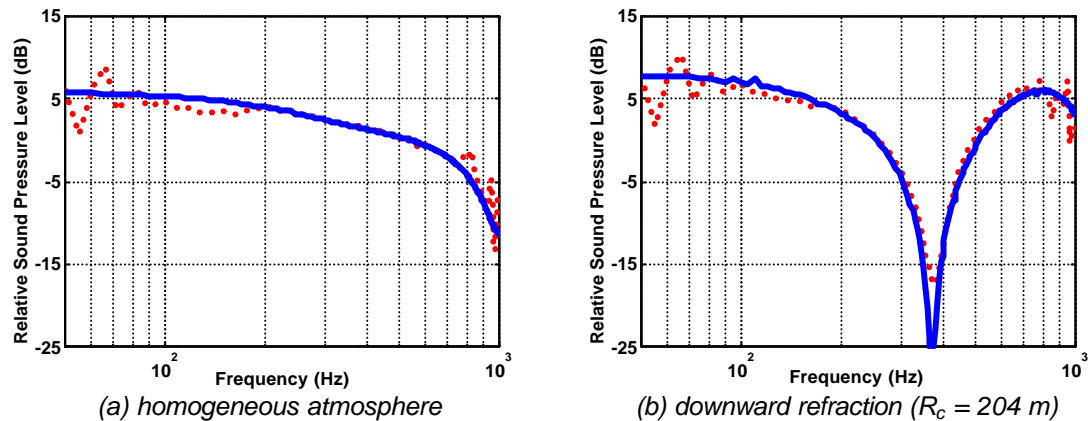


Fig. 10. Comparison theoretical model/ measurements for the surface with the impedance discontinuity, $(\underline{S}, \underline{S}) = (\underline{\mu}, 180 \text{ kNsm}^{-4})$, $z_s = 2 \text{ m}$, $z_r = 2 \text{ m}$, $r = 40 \text{ m}$, distance between source and discontinuity = 28 m, TDS measurements — theoretical model.

All the results show that the agreement between narrow band calculations and measurements is good both in a homogeneous atmosphere and in the presence of downward refraction. Furthermore, they point out the importance of meteorological effects since the interference pattern is significantly affected by refraction within the frequency range of interest.

5- CONCLUDING REMARKS

A case of complex outdoor sound propagation involving an impedance discontinuity has been investigated both in a homogeneous medium and in downward refracting conditions. A theoretical model has been satisfactorily compared to experimental data obtained in laboratory above scale models with curved surfaces. A database of indoor scale models measurements has been built up in order to give a reference for the development of advanced numerical tools for complex outdoor sound propagation. At the time being, further work is in progress for studying more realistic configurations where impedance discontinuity problems are coupled together with uneven topography and meteorological effects. The ultimate goal is to be able to predict sound pressure levels for most typical encountered traffic noise situations.

REFERENCES

1. J. Defrance and Y. Gabillet, "A new analytical method for the calculation of outdoor noise propagation", *Applied Acoustics*, **57**(2), 109-127, (1999)
2. P. Jean, J. Defrance and Y. Gabillet, "The importance of source type on the assessment of noise barriers", *JSV*, **226**(2), 201-216, (1999)
3. E. Premat, Y. Gabillet, "A new boundary element method for predicting outdoor sound propagation and application to the case of a sound barrier in the presence of downward refraction", *JASA*, **108**(6), 2775-2783, (2000)
4. E. Premat, Y. Gabillet, J. Defrance, "Applications of the Meteo-BEM model in downward and upward refracting conditions", 9th International Symposium on Long Range Sound Propagation, TNO, The Hague, 13 p, (2000)
5. E. Premat and J. Defrance, "Theoretical and experimental study of sound propagation for traffic noise", 9th International Congress on Sound and Vibration, Orlando, (2002)
6. M. Almgren, "Simulation by using a curved ground scale model of outdoor sound propagation under the influence of a constant sound speed gradient", *JSV*, **118**(2), 353-370, (1987)
7. D. Habault, "Sound propagation above an inhomogeneous plane : boundary integral equation methods", *JSV*, **100**, 55-67, (1985)
8. J.N.B. Harriott, S.N.B. Chanler-Wilde, D.C. Hothersall, "Long-distance sound propagation over an impedance discontinuity", *JSV*, **148**(3), 365-380, (1991)
9. R. Raspet, G. Baird, W. Wu, "Normal mode solution for low frequency sound propagation in a downward refracting atmosphere above a complex impedance plane", *JASA*, **91**, 1341-1352, (1992)
10. T.F.W. Embleton, "Analogies between nonflat ground and nonuniform meteorological profiles in outdoor sound propagation", *JASA*, **78**(1), S86, (1985)
11. M.E. Delany et E.N. Bazley, "Acoustical properties of fibrous absorbent materials", *Applied Acoustics* **3**, 105-116, (1970)
12. M. Villot, "TDS measuring system developed for a personal computer", *Noise Control Eng. Journal*, **31**, 154-158, (1988)